

## Racemic and enantiomeric effect of tartaric acid on the hydrophilicity of polysulfone membrane

Nilay Sharma\* and Mihir Kumar Purkait

Department of Chemical Engineering, Indian Institute of Technology Guwahati,  
Guwahati- 781039, Assam, India

(Received November 07, 2015, Revised March 04, 2016, Accepted March 09, 2016)

**Abstract.** The enantiomeric and racemic effects of tartaric acid (TA) on the properties of polysulfone (PSn) ultrafiltration membranes were studied in terms of morphology and hydrophilicity (HPCT) of membrane. Asymmetric membranes were prepared by direct blending of polyvinyl pyrrolidone (PVP) with D-TA and DL-TA in membrane casting solution. FTIR analysis was done for the confirmation of the reaction of PVP and TA in blended membranes and plain PSn membranes. Scanning electron microscope (SEM), field emission scanning electron microscope (FESEM) and atomic force microscopy (AFM) were used for analyzing the morphology and structure of the resulting membranes. The membranes were characterized in terms of pure water flux (PWF), hydraulic permeability and HPCT. PWF increased from 52 L/m<sup>2</sup>h to 79.9 L/m<sup>2</sup>h for plain and D-TA containing PSn membrane, respectively. Water contact angle also found to be decreased from 68° to 55°. In Additionally, permeation and rejection behavior of prepared membranes was studied by bovine serum albumin (BSA) solution. A considerable increase in BSA flux (from 19.1 L/m<sup>2</sup>h for plain membrane to 32.1 L/m<sup>2</sup>h for D-TA containing membrane) was observed. FESEM images affirm that the pore size of the membranes decreases and the membrane permeability increases from 0.16 to 0.32 by the addition of D-TA in the membrane. D-TA increases the HPCT whereas; DL-TA decreases the HPCT of PSn membrane. PVP (average molecular weight of 40000 Da) with D-TA (1 wt%) gave best performance among all the membranes for each parameter.

**Keywords:** polysulfone; tartaric acid; hydrophilicity; chirality; polyvinyl pyrrolidone; BSA rejection

### 1. Introduction

In the present era, polymeric materials are widely used for the fabrication of commercial membranes. Mechanical and chemical stability as well as thermal resistance in a broad temperature range are the properties of polymers which makes them suitable for various separation applications (Li *et al.* 2008, Ravanchi *et al.* 2009). Polymeric ultrafiltration (UF) membrane is widely used for Bovine serum albumin (BSA) separation. It is a serum albumin protein derived from milk and also a protein component of whey and blood. BSA, as a serum albumin, has large scale application because of its functional/structural similarity to human serum albumin, lower cost and huge availability (Tsai *et al.* 2011). Thus, BSA separation is exceptionally essential in the field of biotechnology. Several processes like chromatograph, electrophoresis (Chen and Sailor

---

\*Corresponding author, E-mail: [s.nilay@iitg.ernet.in](mailto:s.nilay@iitg.ernet.in)

2011), adsorption (Peng *et al.* 2004) and different membrane processes (Bhattacharjee *et al.* 2012) are available for BSA separation. Among these separation processes ultrafiltration (UF) membrane process is widely used for the separation of BSA. Amongst various polymeric materials such as cellulose acetate, polyamide (PA), polysulfone (PSn), polyacrylonitrile (PAN), polycarbonate (PC), polypropylene (PP), polytetrafluoroethylene (PTFE) and polyvinylidene fluoride (PVDF); PSn is largely used for the fabrication of microfiltration (MF), ultrafiltration (UF) and nanofiltration (NF) membranes. It is because of its wide temperature and pH limits, physicochemical stability, fairly good resistance to chlorine, wide ranges of pore sizes and membrane fabrication is easy in a large variety of modules and configurations (Cheryan 1998). UF is considered as the porous membrane, which has an asymmetric structure with porous top layer (lower surface porosity and smaller pore size) and resulted in an elevated hydrodynamic resistance. The thickness of top layer in an UF membrane is usually less than 1  $\mu\text{m}$  and plays important role in solute separation. In this, process rejection is determined mainly by shape and size of solute relative to the pore size in the membrane and since it is pressure driven membrane separation process, transport of solvent is directly proportional to the applied pressure (Mulder 1991). The major limitation of UF process is membrane fouling which is resulted by increased solute concentration at the surface of membrane either by the adsorption of macromolecules to the internal pore of the membrane or accumulation of solute molecules on surface of membrane and subsequently reduces the life span of membrane and declines the flux. Even though, PSn based UF membrane has numerous advantages but its hydrophobicity is major drawback of this material. These membranes have a tendency to be fouled because of its hydrophobicity (Zhang *et al.* 2008). To overcome this fouling problem many researchers (Sinha *et al.* 2013, Nair *et al.* 2013) have done work for surface modification of PSn based membrane for increasing the hydrophilicity (HPCT) of membrane, consequently reducing the fouling.

Literature shows that even a small amount of organic acid can change the HPCT of polymeric membrane. So, blending of different organic acids with PSn can be used for surface modification and consequently increasing the hydrophilic properties of the membrane. Kumar *et al.* (2013) prepared polysulfone-chitosan blend ultrafiltration membranes with 1 % acetic acid. Their observation resulted with improved antifouling property of bovine serum albumin (BSA) rejection through modified membrane. Xenobiotics removal at different solution pHs was studied by Ghaemi *et al.* (2012b). They investigated the effect of various concentrations (0.25 to 1 wt%) of three different organic acids on the morphology and performance of PSn membrane. They observed that porosity was maximum for 0.5 wt% of all the organic acids in the PSn membrane. Citric acid offered highest retention efficiency of the solutes as compared to other two acids (ascorbic acid and maleic acid). Ghaemi *et al.* (2012a) also studied the effect of amphiphilic fatty acids (palmitic, oleic, and linoleic acid) on the structure and performance of cellulose acetate nano filtration membranes. They observed that addition of palmitic acid represent higher rejection of nitrophenols compared to other fatty acids in all of the solution pHs. Mansourizadeh and Ismail (2010) used Polyethylene glycol (PEG 200) and ethanol, glycerol and acetic acid as the additives in porous PSn hollow fiber membranes for CO<sub>2</sub> absorption. They found that all the additives resulted in enhanced surface porosity. Wei *et al.* (2012) studied the effect of preadsorption of citric acid on surface modification of PSn ultrafiltration membrane. They observed that after modification the membrane surfaces became more hydrophilic and permeability also improved. The modified membranes showed enhanced BSA and PEG retentions and improved antifouling properties with higher flux recovery ratios during filtration of a complex pharmaceutical wastewater. Acrylic acid (AA) was also used with different hydrophilic polymers (Li *et al.* 2013).

Sinha and Purkait (2015) synthesized polyurethane macromolecules (PU) with end capping of citric acid, maleic acid, lactic acid and 4-hydroxy benzoic acid. Membranes blended with PU showed improved pore density, HPCT and pure water flux compared to plain PSn membrane. They also studied the effect of PU on BSA permeation performance of prepared membrane. They observed that BSA flux recovery ratio was higher than the plain membranes for all the modified membranes.

It appears from the literatures review that although lots of works have reported on several organic acids to increase the HPCT of PSn membrane, but no work has been reported on the investigation of enantiomeric and racemic effect of organic acid on the HPCT of polysulfone membrane. The term chirality denotes that the object and its mirror image are not super imposable on each other and are known as enantiomer. Tetrahedral atom (most commonly carbon bonded to four different groups) is the main reason of chirality in organic molecules (Kalsi and Jagtap ISBN 978-81-8487-038-1). Solubility of an enantiomer and racemate is different with each other for chiral compounds. Solubility of D-tartaric acid (D-TA) and DL- tartaric acid (DL-TA) in water is  $5.8 \times 10^2$  g/L and  $1.7 \times 10^2$  g/L at 20°C, respectively (Yalkowsky and He 2010) and the solubility of additives with coagulation bath (i.e., water) affects the HPCT of PSn membrane (Sharma and Purkait 2015). Thus, chirality of TA may affect the HPCT and morphology of PSn membrane. Therefore, in the present study an effort was made to investigate the effects of addition of different amounts of D-TA and DL-TA with PVP into the PSn based membrane. Effects of chirality of TA on the membrane morphology, HPCT, water flux as well as permeation and rejection behaviour were examined and explained well. For the characterization of prepared membranes, morphological parameters were examined by scanning electron microscopy (SEM) for cross sectional view and field emission scanning electron microscope (FESEM) for top surface. Atomic force microscopy (AFM) was used for finding surface roughness parameters. Ion exchange capacity (IEC), equilibrium water content (EWC) and contact angle (CA) measurements were also performed to assess the membrane hydrophilicity.

## **2. Experimental**

### *2.1 Materials and reagents*

Polysulfone (average molecular weight of 30,000 Da) was procured by Sigma-Aldrich Co. USA, and was taken as base polymer in the membrane casting solution. Dimethyl acetamide (DMAc) (supplied by LOBA Chemie, India) was used as solvent. Polyvinyl pyrrolidone (average molecular weight of 40000 Da), D-tartaric acid (pKa = 2.98) and DL-tartaric acid (pKa = 3.03) with average molecular weight of 150 Da for both TAs; were supplied by Otto Chemie Private Limited India. Bovine serum albumin (BSA) with 68000 Da molecular weight was purchased from Otto Chemie Private Limited, India. Chemical reaction of PSn, tartaric acid and PVP is shown in Fig. 1.

### *2.2 Membrane preparation*

Wet phase inversion technique was used for the fabrication of flat film PSn membranes. Constant molecular weight of PVP with D-TA and DL-TA were used as additives and DMAc (79-80 wt%) was used as solvent (Table 1). Membranes with varying compositions were defined as M1, M2, M3, M4 and M5 containing different ratios of organic acids (i.e., D-TA and DL-TA)

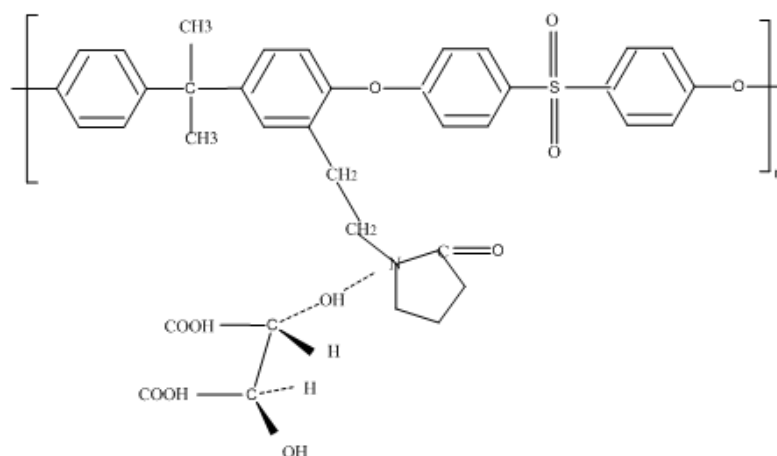


Fig. 1 Chemical reaction of polysulfone, polyvinyl pyrrolidone and tartaric acid

Table 1 Composition of PSn casting solutions of the membranes

Serial No.	Membrane	PSn (wt%)	PVP K-30 (wt%)	DMAc (wt%)	D-TA (wt%)	DL-TA (wt%)
M1	Plain	18	2	80	-	-
M2	D <sub>1</sub> K-30	18	2	79	1	-
M3	D <sub>0.5</sub> K-30	18	2	79	0.5	-
M4	DL <sub>1</sub> K-30	18	2	79.5	-	1
M5	DL <sub>0.5</sub> K-30	18	2	79.5	-	0.5

and solvent (i.e., DMAc). The molecular weight of D-TA and DL-TA was 150 Da. Detailed fabrication procedure is explained in our previous work (Sharma and Purkait 2015).

### 2.3 Characterization of membranes

Permeation experiments and morphological analysis were done for characterizing all the fabricated membranes. Morphological analysis of the prepared membranes was done by SEM, FESEM and AFM. The permeation and rejection capacity of all the membranes was studied in terms of compaction factor (CF), equilibrium water content (EWC), porosity, permeability and rejection (%R) of BSA. Ion exchange capacity (IEC) of the membranes was also studied and water contact angle was measured for finding the HPCT of membrane.

#### 2.3.1 Permeability method and Permeation experiments

Batch experiments were performed at room temperature ( $25 \pm 2^\circ\text{C}$ ) in a dead-end, stainless steel (SS) cell explained in our previous work (Sharma and Purkait 2015). Nitrogen gas of normal purity was used to pressurize the cell to an operating pressure of 208 kPa after the compaction of membrane at 414 kPa. The membrane diameter was same as the SS cell diameter i.e.,  $3 \times 10^{-2}$  m and the permeating solution was collected from the lower side of the cell. Deionized water was used for the compaction of membrane. Fabricated membranes were compacted for 1h at a trans membrane pressure of 414 kPa which was higher than the maximum operating pressure (208 kPa)

for this study. Standard technique was opted for determining the compaction factor (CF) (Chakrabarty *et al.* 2008).

### 2.3.2 Pure water flux (PWF), hydraulic permeability ( $P_m$ ), HPCT and porosity

In pressure driven separation processes, hydraulic permeability of membrane is a key parameter (Chakrabarty *et al.* 2008). Deionized water was allowed to move across the compacted membrane for finding the pure water flux (PWF). Flux values of pure water at different trans membrane pressures were calculated under steady state condition with the help of following equation

$$J_w = \frac{Q}{A\Delta t} \quad (1)$$

where,  $J_w$  is the pure water flux ( $L/m^2$  h),  $Q$  is the volume of permeated water (L),  $A$  is the effective membrane area ( $m^2$ ),  $t$  is the permeation time and  $P_m$  ( $L/m^2$ h kPa) is evaluated from the slope of the plot of  $J_w$  vs  $P$ . Hydraulic permeability was measured using following equation as

$$P_m = \frac{J_w}{\Delta P} \quad (2)$$

Contact angle measurement was done for finding the hydrophilicity of membrane, well discussed in our previous publications (Sharma and Purkait 2015, Sinha and Purkait 2014a).

$$Porosity = \frac{W_w - W_d}{\rho_w V} \quad (3)$$

where  $W_w$  and  $W_d$  are the weight of membrane in wet and dry states, respectively.  $V$  and  $\rho_w$  denote the volume of the membrane and the density of water, respectively.  $W_w$  and  $W_d$  of the membranes were taken on electronic weighing machine. Vacuum oven was used for drying the wet membranes.

### 2.4 Ultrafiltration experiment and Ion exchange capacity (IEC)

UF experiments were performed in the SS cell to study the effect of chirality of tartaric acid on permeate flux and solute separation behavior of the prepared membranes. The protein, Bovine Serum Albumin (BSA), was taken as solute for the filtration experiments. Concentration of solution kept constant at  $1000 \text{ mg L}^{-1}$  for all the filtration experiments. The pH of protein solution affects the separation behavior of it since, acts as a key factor in protein-membrane interface (Higuchi *et al.* 1993). BSA solution (molecular weight 68000 Da) pH was taken at five values: 3, 4.8 (i.e., at isoelectric point), 7, 8 and 10.3. BSA rejection ratio was measured by the following equation

$$R\% = \frac{(1 - C_p)}{C_f} \times 100 \quad (4)$$

where,  $C_f$  concentrations in the feed and  $C_p$  concentrations in the permeate in g/L, respectively. Concentration was measured for 5 h, the permeate sample was collected at every 1 h interval of ultrafiltration. UV-vis spectrophotometer (Perkin-Elmer Precisel, Lamda-35) was used for finding the concentrations of BSA in permeate. The IEC of the PSn-(D-TA or DL-TA) membranes was

determined by the back titration method. The measured IEC of the PSn/DMAc/PVP/(D-TA or DL-TA) membranes was calculated by the following equation (Yan *et al.* 2012)

$$IEC = \frac{(V_b - V_s)C_{HCl}}{W_{dry}} \times 1000 \quad (5)$$

Where,  $V_b$  and  $V_s$  are the consumed volumes (L) of the NaOH solution for the blank sample and the PSn/DMAc/PVP/(D-TA or DL-TA) membrane sample, respectively.  $W_{dry}$  is the weight (g) of dry membrane and  $C_{HCl}$  is the concentration of HCl solution (M).

### 3. Results and discussion

#### 3.1 FTIR-ATR analysis of different membranes

Fig. 2 represents the FTIR-ATR spectra of membranes M1, M2, M3, M4 and M5. Peak at  $693 \text{ cm}^{-1}$  is the characteristic band of the plane aromatic C-H bond in PSn membrane. Stretching at  $845 \text{ cm}^{-1}$  represents S-O-C group, symmetric and asymmetric stretching of sulfonate groups are presented by peaks  $1144 \text{ cm}^{-1}$  and  $1243 \text{ cm}^{-1}$ , respectively. Peak at  $2905 \text{ cm}^{-1}$  shows the presence of TA with C-H stretching of methyl group. The strong absorption peaks between  $1485\text{-}1595 \text{ cm}^{-1}$  are related to the stretching of benzene ring skeletal. Peak found at  $1665 \text{ cm}^{-1}$  in FTIR-ATR spectra of PSn is related to amide C = O groups of PVP molecules which added as the pore former to PSn casting solution.

#### 3.2 Morphological study

AFM images were used for determining the surface roughness parameters. Field emission scanning electron microscope (FESEM) was used for finding the size and shape of the pores of

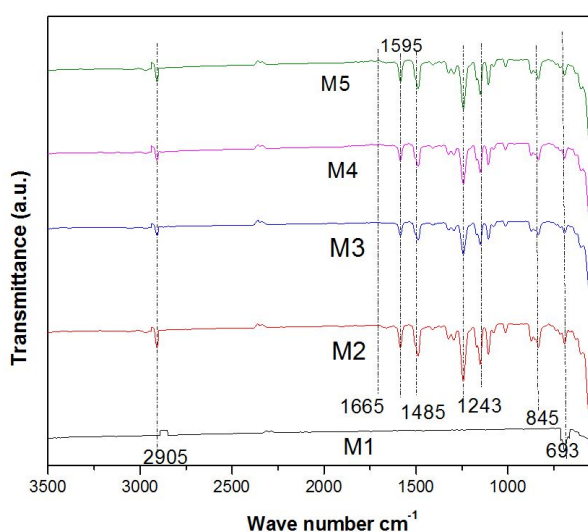


Fig. 2 FTIR-ATR spectra of M1, M2, M3, M4 and M5 membranes

different membrane. Higher magnification was needed for top surface images for finding the size of pores, so these images were taken by FESEM. In contrast, the cross-sectional morphology of the membranes was analyzed by SEM images, since lower magnification was sufficient for knowing the cross sectional morphology of the pores.

### 3.2.1 SEM analysis

SEM images of the cross-sectional view of all the 5 membranes prepared with constant molecular weight of PVP with D-TA and DL-TA (Table 1) were depicted in Fig. 3 (left column). It was confirmed from those images that membranes prepared by wet phase inversion technique were asymmetric porous structure. Membranes depict a dense top layer and a porous sub-layer, which was almost common for all the membranes. However, the thickness of top layer changed with the composition and ingredients of the membranes. The porosity of the prepared membranes increases with different concentrations of TA this information may be explained by the fact: (i) interactions got reduced between polymer chains because of the interactions between TA molecules and polymer; as well as (ii) reduced solvent (DMAc) outflow and increased non-solvent (water) inflow due to the hydrophilicity of TA added to the casting solution (Kim and Lee 2003). Hence, membranes with higher porosity were formed since the rate of demixing of the casting solution increases (Wang *et al.* 1998). Fig. 3 (left column) depicts the cross sectional images of plain membrane and membranes containing PSn/PVP/D-TA/DMAc as well as PSn/PVP/DL-TA/DMAc. They made it confirm that pores were more regular and dense top layer thickness got reduced by the addition of D-TA as compared to plain and PSn/PVP/DL-TA/DMAc membrane. This fact can also be explained by the concentration of DMAc in coagulation bath. The amount of DMAc was found about 152  $\mu\text{g/L}$  and 84  $\mu\text{g/L}$  for M2 and M4 membrane, respectively. The porous sub-layer seems to possess finger-like structure. Since, DMAc is highly soluble in water and shows high interactive affinity with water, instantaneous demixing occurs during membrane preparation by wet phase inversion method which further results in the creation of finger like structure in the sub-layer of the fabricated membranes (Mulder 1991). Throughout the process, the concentration of non-solvent in the polymer solution slowly increases until the demixing gap is reached (Duarte *et al.* 2012). In the ternary system a miscibility gap is present with metastable regions (El-Gendi *et al.* 2012). The liquid-liquid phase boundary is known as binodal. In thermodynamics, the spinodal is defined as the limit of stability of a solution it denotes the boundary of absolute instability of a solution to decompose into multiple phases (Blanco *et al.* 2006). With reference to the phase separation theory, three modes of phase separation can occur in such ternary system: (i) nucleation and growth of the polymer lean phase; (ii) spinodal phase separation and nucleation; and (iii) growth of the polymer rich phase. As polymer is one of the components in the ternary system and solidification of this part in the system (casting solution) can take place.

### 3.2.2 FESEM image analysis

Fig. 3 (right column) depicts the FESEM images for the top surface of fabricated. Spinodal demixing may be the cause of formation of dense top surface. This is attributed to the fact that during formation of top layer the diffusion process between coagulation medium i.e., deionized water and casting or polymer solution was so fast to become highly unstable and cross the spinodal curve (Kimmerle and Strathmann 1990, Reuvers and Smolders 1987). This gives a top surface with to a large extent of interconnected pores. These interconnected pores can be taken as a continuous polymer or PSn lean (i.e., PVP-TA rich) phase tangled by a continuous PSn rich (i.e., PVP-TA lean) phase. Average pore size by FESEM images was calculated using Image J software

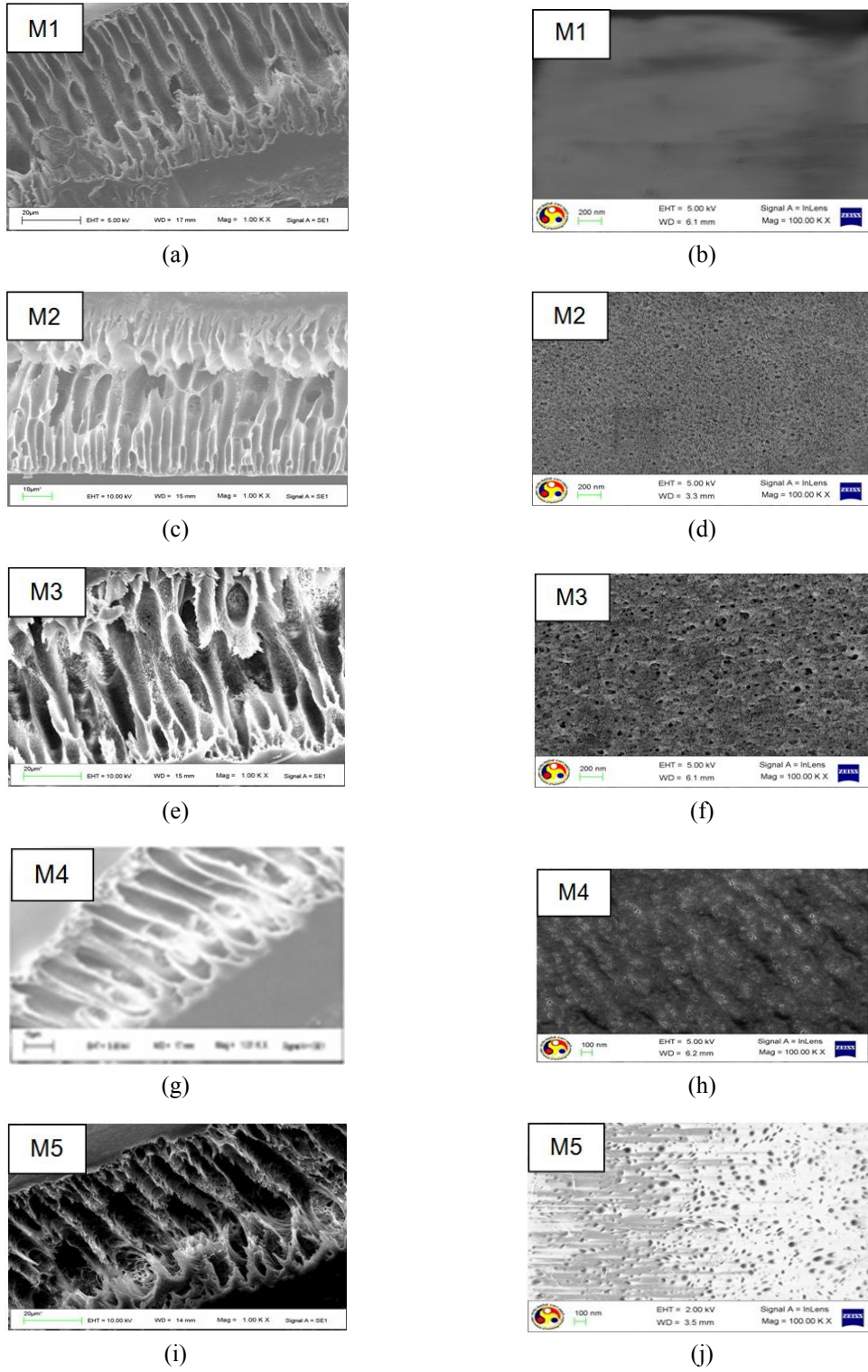


Fig. 3 SEM and FESEM images of membrane cross section and top Surface for M1, M2, M3, M4 and M5

(Hand *et al.* 2009). It was calculated as 27.96 nm, 21.17 nm and 36.43 nm for M1, M2 and M4, respectively. These pore size values made it confirm that all the membranes were in UF range. It was confirmed that addition of DL-TA increased the pore size whereas; addition of D-TA reduced the pore size of the membranes. This fact consequently affects the rejection behavior of the membranes.

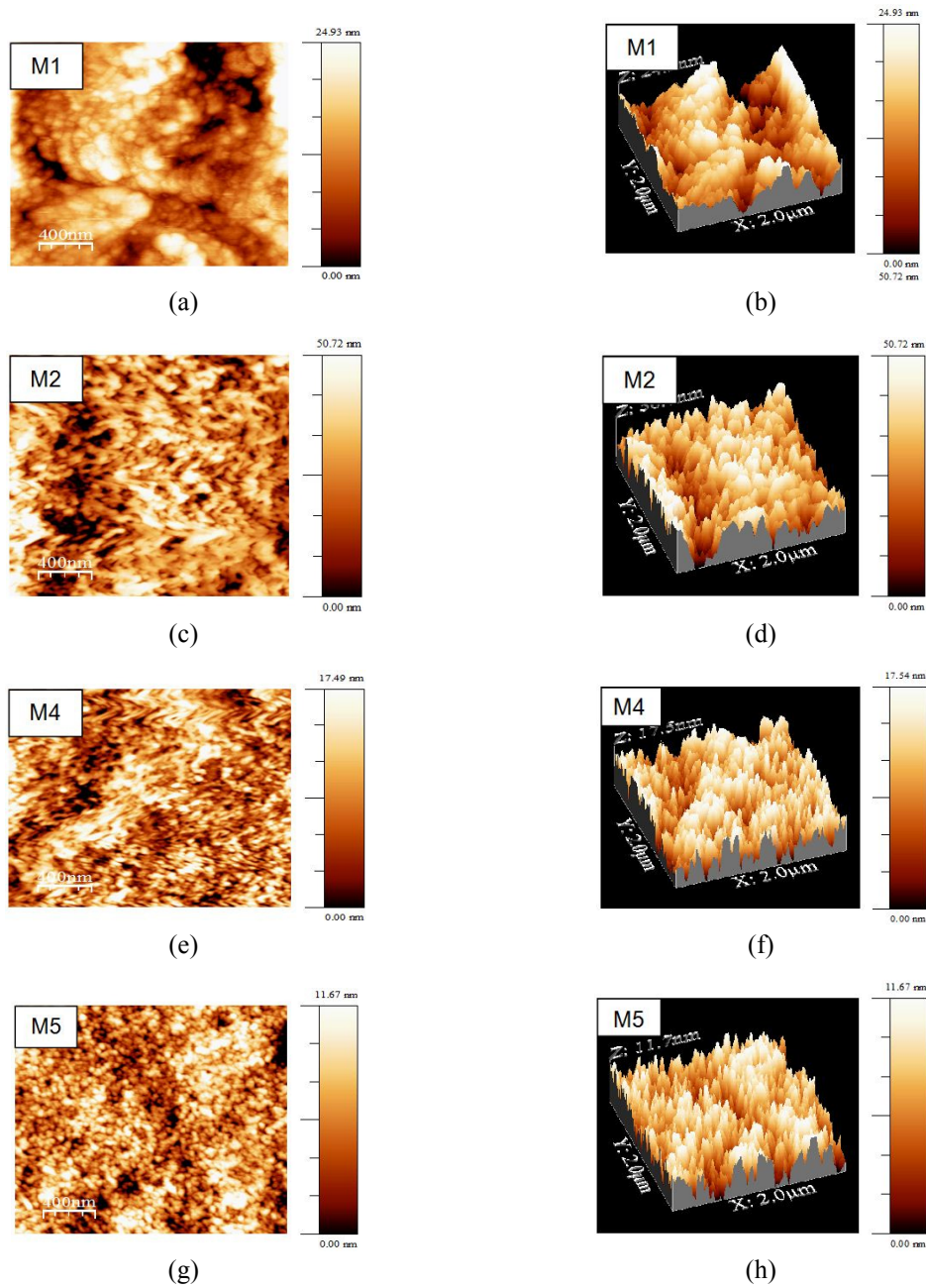


Fig. 4 AFM (2D and 3D) images of membranes

### 3.2.3 AFM analysis

Surface morphology and roughness of the membranes were analyzed by atomic force microscopy (AFM). Small squares of membranes (Approximately 1.5 cm<sup>2</sup>) were taken and analyzed. Fig. 4 depicts the AFM images of the M1, M2, M4 and M5 membranes. Average height ( $S_z$ ), root mean square (RMS) roughness ( $S_q$ ) and average roughness ( $S_a$ ) were measured. RMS roughness was increased with the addition of D-TA and decreased with DL-TA. Further it was found that D-TA containing membranes show more RMS roughness than DL-TA containing membranes (Table 2). It may be due to the fact that porosity increasing with the addition of D-TA as compared to DL-TA. Table 2 shows different surface roughness parameters. The contact angle also decreased with the addition of D-TA and was measured as 68°, 55°, 59°, 71° and 73° for M1, M2, M3, M4 and M5, respectively. Number of pores also increased by blending of D-TA. It indicates increasing HPCT with addition of D-TA in this study. Between D-TA and DL-TA, enantiomeric TA increased the HPCT for example contact angle for M2 and M4 was 55° and 71°, respectively. This is due to more solubility of D-TA in water than DL-TA. Thus, more pores were formed by the addition of D-TA.

### 3.2.4 Permeability

The pore size, number of pores and area of pores for each of the 5 membranes were calculated by permeability method (Sharma and Purkait 2015). The pure water flux was varying at altered pressure, i.e., at higher pressure the flux was higher and porosity also depends on the applied pressure. Since, by applying more pressure smaller pores will be opened. Lesser number of bigger pores mainly plays the role in the permeation hence total membrane performance increases by increasing the permeability. However, solute rejection may be affected as the pore size gets increased. Table 2 also shows the results of permeation experiments. It was noted that with increasing strength of the D-TA, number of pores increases consequently more permeable membrane was found. Number of pores per unit area ( $N_t$ ) were found to be increased from  $2.66 \times 10^{12} \text{ m}^{-2}$  to  $4.08 \times 10^{12} \text{ m}^{-2}$  for M1 and M2, respectively by the addition of D-TA. Increasing the concentration of D-TA from 0.5 g to 1g also resulted in increased pore numbers from  $2.85 \times 10^{12} \text{ m}^{-2}$  to  $4.08 \times 10^{12} \text{ m}^{-2}$  for membrane M3 and M2, respectively.

## 3.3 Permeation studies

### 3.3.1 Effect of chirality of TA on CF

Fig. 5 depicts the ternary phase diagram showing the solubility of the racemic species for conglomerate and racemic compound. Fig. 5(a) corresponds to the eutectic behavior of

Table 2 Surface roughness and other characterization parameters of the membranes

Serial No.	Membrane	Mean pore size (nm)	Roughness parameters			Pore area $A_t \times 10^9$ (m <sup>2</sup> )	Pore number $N_t \times 10^{-8}$ (m <sup>2</sup> )	Permeability (L/m <sup>2</sup> h kPa)
			$S_a$ (nm)	$S_q$ (nm)	$S_z$ (nm)			
M1	Plain	2.8	4.7	5.8	12.4	8.64	3.51	0.16
M2	D <sub>1</sub> K-30	2.48	9.9	12.1	25.5	8.73	4.52	0.32
M3	D <sub>0.5</sub> K-30	2.49	5.2	7.6	13.5	8.6	4.43	0.24
M4	DL <sub>1</sub> K-30	2.91	3.5	4.2	8.8	4.57	1.72	0.13
M5	DL <sub>0.5</sub> K-30	3.1	2.3	2.8	5.9	3.89	1.29	0.08

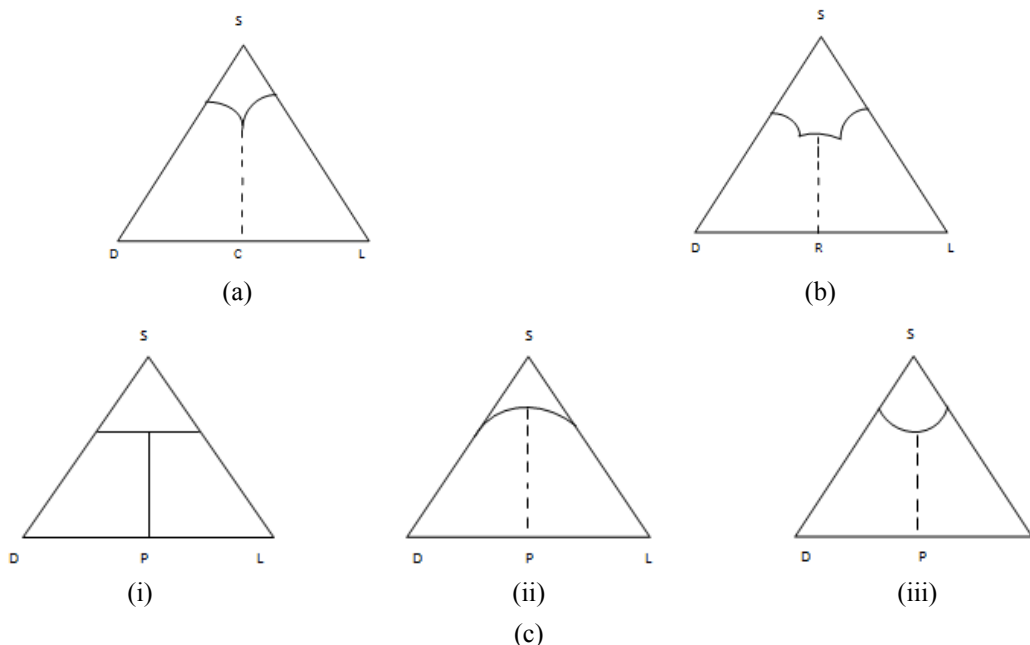


Fig. 5 Ternary phase diagram showing the solubility of the racemic species: (a) conglomerate; (b) racemic compound (R); (c) pseudoracemate (P) ((i) ideal; (ii) positive deviations; (iii) negative deviations, D and L represent the enantiomers, S represents the solvent and R represents the racemic species)

enantiomers. Fig 5(b) depicts the representative ternary phase diagram for the solubility of a racemic compound and shows that most of the racemic compounds have lower solubility than pure enantiomer. Fig. 5(c) presents the ideal, positive deviation and negative deviation conditions of pseudoracemate. Racemic mixture of the enantiomers is less soluble than the pure enantiomer (Yalkowsky and He 2003). It may be due to the fact that racemic forces reduce the solubility of racemic mixture. Both the enantiomers show same solubility in a particular solvent at constant temperature. Compaction factor (CF) is an important factor for describing the structure of the membrane, especially for the membrane sub-layer. Increased CF shows the presence of large number of macrovoids in the sublayer. Initially all the 5 membranes were compacted for 1h at 414 kPa and after that pure water flux (PWF) was collected for next 1h at the operating pressure of 208 kPa. Fig. 6 shows the PWF after compaction and BSA flux after PWF. It was noticed that both PWF and BSA flux was highest for both the D-TA containing membranes whereas flux was least for both the DL-TA containing membranes. This was due to less solubility of DL-TA than D-TA. Racemic forces reduce the solubility of DL-TA (i.e., racemic mixture) in coagulation bath and consequently less porous membrane. Since, Levo-TA (another enantiomer of TA) has same solubility in water as D-TA shows; it gave the same permeation and rejection behavior with a particular molecular weight of PVP in a PS<sub>n</sub> membrane.

### 3.3.2 Compaction behavior of membranes

The effect of compaction time on PWF for all the 5 membranes (i.e., M1, M2, M3, M4 and M5) is shown in Fig. 7. Flux was found as 84.76 L/m<sup>2</sup>h, 161.03 L/m<sup>2</sup>h and 53.19 L/m<sup>2</sup>h for M1, M2 and M4, respectively. Flux decreased drastically up to 0.33 h; finally attain a steady state after

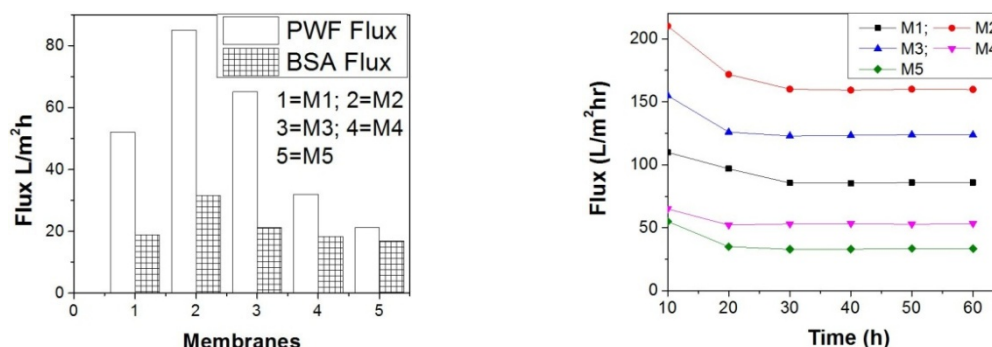


Fig. 6 PWF and BSA flux for all the membranes after Fig. 7 Flux profile during compaction at 414 kPa compaction (at 414 kPa), at 208 kPa and 1 h

around 0.33 h. It was observed that the steady state PWF decreased with addition of DL-TA whereas, it increased by the addition of D-TA for all the membranes. For example, the steady state flux increases from around 84.76 L/m<sup>2</sup>h to 161.03 L/m<sup>2</sup>h, when D-TA<sub>1</sub> was added to the membrane whereas it decreases from 84.76 L/m<sup>2</sup>h to 53.19 L/m<sup>2</sup>h by the addition of DL-TA<sub>1</sub> to the membrane. The CF for the membranes is presented in Table 3. It is seen that for PSn/DMAc/PVP/D-TA membranes possess highest CF than DL-TA containing membranes as well as without any acid containing membrane. The CF was calculated as 1.74, 1.41, 1.48, 1.81 and 1.96 for M1, M2, M3, M4 and M5, respectively. This may be attributed to the fact that addition of two additives into the membrane casting solution can either extra enlarge or in addition suppress the macrovoids present in the membrane beneath the top layer (i.e., sublayer) depending on their molecular weight and the type of solvent used (Machado *et al.* 1999).

### 3.3.3 Effect of the addition of D-TA and DL-TA on PWF and hydraulic permeability

Fig. 8 depicts the effect of addition of D-TA and DL-TA or enantiomeric and racemic effect of organic acid on PWF at different trans membrane pressures (TMP). PWF (calculated using Eq. (1)) increases almost linearly with increase in TMP, for all the membranes. It was also found that the PWF decreased by addition of DL-TA in membrane at a certain pressure, these observations support the results of the compaction study (Fig. 7). For example, at 200 kPa, the PWF decreases from 57.79 Lm<sup>-2</sup>h<sup>-1</sup> to 19.97 Lm<sup>-2</sup>h<sup>-1</sup> for membrane M2 and M4, respectively.

Hydraulic resistance ( $R_m$ ) is also an important consideration for finding the HPCT of membranes. It was observed that hydraulic resistance ( $R_m$ ) was decreased by the addition of D-TA. Whereas, it was found to be increased by the addition of DL-TA.  $R_m$  for PSn/DMAc/PVP system was calculated as  $2.38 \times 10^{12}$ ,  $1.46 \times 10^{12}$ ,  $1.9 \times 10^{12}$ ,  $3.89 \times 10^{12}$  and  $5.8 \times 10^{12}$  (m<sup>-1</sup>) for M1, M2, M3, M4 and M5, respectively. Enhanced hydraulic resistance and subsequently decline in flux with addition of DL-TA may be due to the solubility of it in water, as it is less soluble than D-TA, it remains inside the pore with PVP and reduced the sublayer pore size however the top layer pores were bigger but pores present in per unit square area were less on top layer as shown in FESEM images (Fig. 3, right column). The decrease in hydraulic resistance and therefore elevated flux by the addition of D-TA may due to the fact that it is highly soluble in water and since having less molecular size it creates smaller pores on the top layer. It does not remain inside the pores with or without PVP and increased the sublayer pore size thus, pores present in per square area on the top surface were more as shown in FESEM images (Fig. 3, right column).

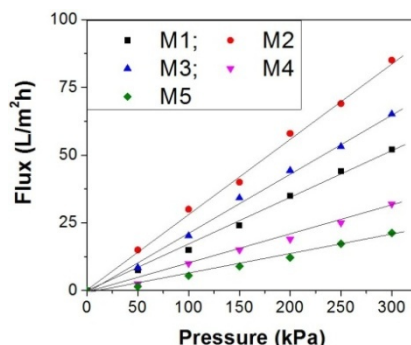


Fig. 8 Effect of transmembrane pressure on PWF

### 3.4 Characterization of membrane by EWC, porosity and HPCT

#### 3.4.1 Effect of the addition of D-TA and DL-TA on EWC

Standard equation (Chakrabarty *et al.* 2008) was used for finding the EWC of all the membranes and calculated values are presented in Table 3. The EWC has a close link with PWF. It was observed from the calculations that by the addition of D-TA, EWC increased from 65.0 to 69.0 and 66.5 for M1 to M2 and M3, respectively. This increasing tendency confirms the occurrence of increasing number of pores in the membrane with addition of D-TA (Table 2). Water molecules are accommodated into the nano metric pores formed on the skin layer as well as macrovoids in the sublayer of the membrane (Sivakumar *et al.* 1999). However, addition of DL-TA into the membrane matrix reduced the EWC from 65.0 to 63 and 59.9 for M1, M4 and M5 the PVP molecule and in membrane matrix and during wet phase inversion method they got released from the membrane and mostly from the top surface resulting in the disturbance of polymer network. On the other hand, DL-TA molecules could not disperse into the coagulation bath. Since, their solubility in water is less than D-TA. It is crystal clear from the SEM images that the length of sublayer got reduced for all the DL-TA containing membranes. M2 shows the highest EWC. Hydrogen bonds between PVP and TA may first formed during preparation of membrane casting solution (Fig. 1) and have been broken during immersion of membrane into the coagulation bath and some TA molecules came out to the surface of membrane.

#### 3.4.2 Effect of addition of D-TA and DL-TA on porosity and HPCT

Role of HPCT and porosity of the membrane is undoubtedly significant in membrane performance. Surface HPCT is principally described by the contact angle measurement (Farbod

Table 3 Values of some characterization parameters of all the membranes

Membrane	EWC (%)	$R_m \times 10^{-12}$ (m <sup>-1</sup> )	CF	IEC	PWF (L/m <sup>2</sup> h)	Contact angle (°)
Plain	65.0	2.38	1.74	1.47	52	68
D <sub>1</sub> K-30	69	1.46	1.41	1.85	79.9	55
D <sub>0.5</sub> K-30	66.5	1.9	1.48	1.80	65.1	59
DL <sub>1</sub> K-30	63	3.89	1.81	1.75	32	71
DL <sub>0.5</sub> K-30	59.9	5.8	1.96	1.59	21.12	73

and Rezaian 2012). Generally it is a common phenomenon, that smaller the contact angle values higher the HPCT. Porosity of the membranes was measured using Eq. (3). Contact angle of membranes without any kind of TA and with different concentration of D-TA and DL-TA are shown in Table 3. It can be seen from Table 3 that contact angle decreased and porosity increased with the addition of D-TA and vice versa for DL-TA. The contact angle for M1, M2, M3, M4 and M5 was 68°, 55°, 59°, 71° and 73°, respectively. Similarly, porosity for M1 and M2 was 0.35 and 0.38, respectively. Increase in porosity blending with D-TA and decrease in porosity by the mixing of DL-TA may be due the fact that solubility of D-TA and DL-TA, as discussed in the previous section. The porosity change can be explained with the help of kinetic and thermodynamic consideration (Mulder 1991).

### 3.5 Ultrafiltration of BSA

Trans-membrane pressure is a key factor for finding the characteristic of flux other than that, structure of the membrane and the properties of the feed solution play important role in permeation and rejection of solute through the membranes, specially its pH. So, fabricated UF membranes were also tested at different pH in permeation experiment by measuring flux and rejection capacity.

#### 3.5.1 Effect of molecular weight of PVP and concentration of D-TA and DL-TA on BSA rejection

Fig. 9 shows the effect of addition of D-TA and DL-TA on the rejection of BSA at normal pH (i.e., pH 7). It was confirmed that BSA rejection increased by the addition of D-TA and it decreased by the addition of DL-TA. So, addition of different quantities of D-TA and DL-TA with PVP (i.e., 40000 Da) was studied and by increasing the concentration of D-TA and DL-TA the rejection was found to be increased, it may be attributed to the reason that after addition of additives into the PSn casting solution, hydrophilic functional groups of both TA's were increased. On the other hand, addition of DL-TA reduced the rejection because of the formation of larger pores on the top surface of membranes. For example rejection (%) for M1, M2, M3, M4 and M5 was 86%, 90.5%, 87.8%, 81.1% and 78.2%, respectively. Moreover, addition of different forms of organic acid altered the membrane morphology as well as skin-layer thickness (Fig. 3) and hence higher porosity was formed by the addition of D-TA and reduced porosity by the addition of DL-TA. Varying morphology possesses a significant control over increment of PWF of the modified membranes.

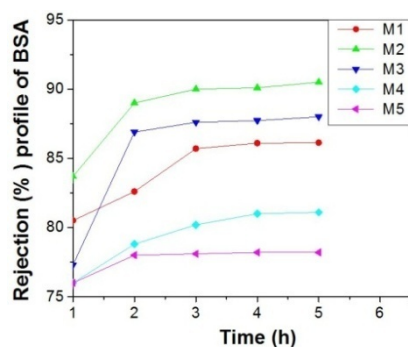


Fig. 9 BSA Rejection profile at normal pH

### 3.5.2 Effect of pH of BSA

Fig. 10 depicts the flux through membrane M2 at different pH. Maximum flux was observed at pH 10 and that of minimum at pH 3. It may be attributed to the fact that at basic condition (pH 10), there was a less charge density at the surface of the membrane because  $H^+$  ions of the TA reacted with  $OH^-$  ions present in the feed solution. On the other hand, at pH 3, there was a highest  $H^+$  ion density on the top layer of the membrane which obstructed the permeation causing less flux. At pH 7, moderate flux was found because at this pH, BSA molecules have net negative charge and electrostatic repulsion causes more expansion than iso-electric point (IEP) of BSA solution (i.e., pH 4.8) (Fane *et al.* 1981, Musale and Kulkarni 1997, Ghosh and Cui 1998). At IEP, BSA molecules are least soluble and they do not have charge in this condition. The BSA molecule accumulated in its most compact size on the membrane surface and reduces the permeation (Fane *et al.* 1981). This compact layer is mostly responsible for lower flux and higher BSA rejection other than at pH 3. It can be seen from Fig. 11 that at different pH values flux was slightly decreased after 1 h and get nearly constant after 3 h. IEC is used for knowing the intensity of charge in the membranes and also fouling behavior. Table 3 illustrates the IEC of different membranes. IEC for membranes M1, M2, M3, M4 and M5 was 1.47, 1.85, 1.80, 1.75 and 1.59, respectively. It clearly shows that IEC was increasing by the addition of D-TA and DL-TA in the membranes. This fact can be explained with the help of ionization behavior of TA present in membrane matrix of M2, M3, M4 and M4. Variation in BSA solution flux at different pH may be described by protonation and deprotonation potential of D-TA, as its acid dissociation constant  $pK_a$  is about  $\sim 2.98$ . Thus, carboxylic group of TA was deprotonated to carboxylate ions. These carboxylate ions offer high charge density in the PVP/D-TA blended membranes. Loss of flux with decreasing pH may be because of the electro viscous effect (Sinha and Purkait 2014b). Fig. 11 depicts the rejection of BSA solution at different pH for membrane M2. Rejection of BSA molecules with the pH was found in the sequence of  $8.0 > 7.0 > 4.8 > 10 > 3.0$ . Rejection was found to be lowest at lowest pH (i.e., pH 3) and slightly higher at pH 10. This may be because of the fact that pores become bigger at extreme acidic and extreme basic condition due to collapse of PVP/D-TA molecules and thus fallout in lower rejection of BSA (Sinha and Purkait 2014b). Proteins are most soluble at high and low pH. (Cheryan 1998). Hence, BSA molecules passed through the pore resulted in lowest rejection. At IEP, BSA is least soluble and hence accumulated on the surface of membrane and results in lowering flux and moderate rejection than pH 3 and pH 10. The higher rejection of BSA molecules in basic and neutral solution condition

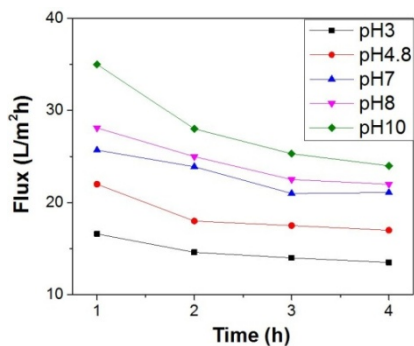


Fig. 10 Effect of pH on BSA flux for M2 membrane

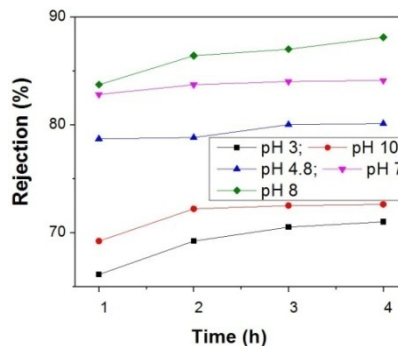


Fig. 11 Effect of pH on BSA rejection for M2 membrane

(pH 8 and pH 7) might be explained by the fact that at these pHs feed solution had net negative ions and deprotonation of D-TA was occurred and caused robust electrostatic charge repulsion between negative charges of the membrane surface and negative BSA molecules.

#### 4. Conclusions

Effects of addition of D-TA and DL-TA on the morphology such as number of pores, pore area and average pore size were investigated in detail. Effects of wt% of both the TAs in membrane morphology were measured and following observations were made:

- (i) Maximum porosity was observed for PVP with D-TA (1 wt%). Porosity was found to be increased by the addition of D-TA, however, it got reduced by the addition of DL-TA.
- (ii) Size of pores on the membrane surface was increased with DL-TA but reduced by the addition of D-TA which was confirmed by the FESEM images.
- (iii) The PWF, hydraulic permeability, EWC, porosity and HPCT were increased and hydraulic resistance  $R_m$  was decreased by the addition of D-TA and vice versa with DL-TA.
- (iv) IEC of the membranes was improved by the addition of both D-TAs and DL-TA. CF was increased by D-TA and reduced by DL-TA. It can be seen in SEM photographs that by the addition of D-TA finger like structure became clear and larger macrovoids were formed in sublayer.
- (v) At normal solution pH (i.e., pH 7), BSA rejection was found maximum for M2 membrane. Further study the effect of pH on the M2 membrane revealed the fact that BSA flux was increased with increase in pH and the order of pH with respect to the increment of flux was  $10 > 8 > 7 > 4.8 > 3$ . On the other hand, the order of pH with respect to the increased BSA rejection was  $8 > 7 > 4.8 > 10 > 3$ .

Finally, it may be concluded that racemic and enantiomeric effect plays an important role in the morphology, HPCT and rejection behavior of membranes.

#### Acknowledgment

This work is partially supported by a grant from the Indian National Science Academy (INSA), New Delhi. Any opinions, findings and conclusions expressed in this article are those of the authors and do not necessarily reflect the views of INSA, New Delhi.

#### References

- Bhattacharjee, S., Dong, J., Ma, Y., Hovde, S., Geiger, J.H., Baker, G.L. and Bruening, M.L. (2012), "Formation of high-capacity protein-adsorbing membranes through simple adsorption of poly(acrylic acid)-containing films at low pH", *Langmuir*, **28**(17), 6885-6892.
- Blanco, J.F., Sublet, J., Nguyena, Q.T. and Schaetzel, P. (2006), "Formation and morphology studies of different polysulfones-based membranes made by wet phase inversion process", *J. Membr. Sci.*, **283**(1-2), 27-37.
- Chakrabarty, B., Ghoshal, A.K. and Purkait, M.K. (2008), "Effect of molecular weight of PEG on membrane morphology and transport properties", *J. Membr. Sci.*, **309**(1-2), 209-221.
- Chen, M.Y. and Sailor, M.J. (2011), "Charge-gated transport of proteins in nanostructured optical films of

- mesoporous silica”, *Anal. Chem.*, **83**(18), 7186-7193.
- Cheryan, M. (1998), *Ultrafiltration and Microfiltration Handbook*.
- Duarte, A.R.C., Mano, J.F. and Reis, R.L. (2012), “The role of organic solvent on the preparation of chitosan scaffolds by supercritical assisted phase inversion”, *J. Supercrit. Fluid.*, **72**(12), 326-332.
- El-Gendi, A., Abdalla, H. and Ali, S. (2012), “Construction of ternary phase diagram and membrane morphology evaluation for polyamide/formic acid/water system Australian”, *J. Basic Appl. Sci.*, **6**(5), 62-68.
- Fane, A.G., Fell, C.J.D. and Waters, A.G. (1981), “The relationship between membrane surface pore characteristics and flux for ultrafiltration membranes”, *J. Membr. Sci.*, **9**(3), 245-262.
- Farbod, M. and Rezaian, S. (2012), “An investigation of super-hydrophilic properties of TiO<sub>2</sub>/SnO<sub>2</sub> nanocomposite thin films”, *Thin Solid Films*, **520**(6), 1954-1958.
- Ghaemi, N., Madaeni, S.S., Abdolhamid, A., Rajabi, H., Daraei, P. and Falsafi, M. (2012a), “Effect of fatty acids on the structure and performance of cellulose acetate nanofiltration membranes in retention of nitroaromatic pesticides”, *Desalination*, **301**(17), 26-41.
- Ghaemi, N., Madaeni, S.S., Alizadeh, A., Daraei, P., Badiie, M.M.S., Falsafi, M. and Vatanpour, V. (2012b), “Fabrication and modification of polysulfone nanofiltration membrane using organic acids: Morphology, characterization and performance in removal of xenobiotics”, *Sep. Purif. Technol.*, **96**(14), 214-228.
- Ghosh, R. and Cui, Z.F. (1998), “Fractionation of BSA and lysozyme using ultrafiltration: effect of pH and membrane pretreatment”, *J. Membr. Sci.*, **139**(1), 17-28.
- Hand, A.J., Sun, T., Barber, D.C., Hose, D.R. and MacNeil, S.J. (2009), “Automated tracking of migrating cells in phase-contrast video microscopy sequences using image registration”, *J. Microsc. Microsc.*, **234**(1), 62-79.
- Higuchi, A., Ishida, Y. and Nakagawa, T. (1993), “Surface modified polysulfone membranes-separation of mixed proteins and optical resolution of tryptophan”, *Desalination*, **90**(1-3), 127-136.
- Kalsi, P.S. and Jagtap, S. (2013), *Pharmaceutical Medicinal and Natural Product Chemistry*, Narosa Publishing House PVT. LTD. ISBN 978-81-8487-038-1
- Kim, I.C. and Lee, K.H. (2003), “Effect of various additives on pore size of polysulfone membrane by phase-inversion process”, *J. Appl. Polym. Sci.*, **89**(9), 2562-2566.
- Kimmerle, K. and Strathmann, H. (1990), “Analysis of the structure-determining process of phase inversion membranes”, *Desalination*, **79**(2-3), 283-302.
- Kumar, R., Isloor, A.M., Ismail, A.F., Suraya, A. and Matsuura, T. (2013), “Polysulfone–Chitosan blend ultrafiltration membranes: Preparation, characterization, permeation and antifouling properties”, *RSC Advances*, **3**(21), 7855-7861. DOI: 10.1039/C3RA00070B
- Li, G.M., Feng, C., Li, J.F., Liu, J.Z. and Wu, Y.L. (2008), “Water vapor permeation and compressed air dehydration performances of modified polyimide membrane”, *Sep. Purif. Technol.*, **60**(3), 330-334.
- Li, J., Nie, S., Wang, L., Sun, S., Ran, F. and Zhao, C. (2013), “One-pot synthesized poly(vinyl pyrrolidone-co-methyl methacrylate-co-acrylic acid) blended with poly(ether sulfone) to prepare blood-compatible membranes”, *J. Appl. Poly. Sci.*, **130**(6), 4284-4298. DOI: 10.1002/app.39463
- Machado, P.S.T., Habert, A.C. and Borges, C.P. (1999), “Membrane formation mechanism based on precipitation kinetics and membrane morphology: Flat and hollow fiber polysulfone membranes”, *J. Membr. Sci.*, **155**(2), 171-183.
- Mansourizadeh, A. and Ismail, A.F. (2010), “Effect of additives on the structure and performance of polysulfone hollow fiber membranes for CO<sub>2</sub> absorption”, *J. Membr. Sci.*, **348**(1-2), 260-267.
- Mulder, M. (1991), *Basic Principles of Membrane Technology*, Kluwer Academic Publishers; Dordrecht, The Netherlands.
- Musale, D.A. and Kulkarni, S.S. (1997), “Relative rates of protein transmission through poly (acrylonitrile) based ultrafiltration membranes”, *J. Membr. Sci.*, **136**(1-2), 13-23.
- Nair, A.K., Isloor, A.M., Kumar, R. and Ismail, A.F. (2013), “Antifouling and performance enhancement of polysulfone ultrafiltration membranes using CaCO<sub>3</sub> nanoparticles”, *Desalination*, **322**, 69-75.
- Peng, Z.G., Hidajat, K. and Uddin, M.S. (2004), “Adsorption of bovine serum albumin on nanosized magnetic particles”, *J. Colloid Interface Sci.* **271**(2), 277-283.

- Ravanchi, M.T., Kaghazchi, T. and Kargari, A. (2009), "Application of membrane separation processes in petrochemical industry: a review", *Desalination*, **235**(1-3), 199-244.
- Reuvers, J. and Smolders, C.A. (1987), "Formation of membranes by means of immersion precipitation. Part II. The mechanism of formation of membranes prepared from the system cellulose acetate– acetone–water", *J. Membr. Sci.*, **34**(1), 67-86.
- Sharma, N. and Purkait, M.K. (2015), "Preparation of hydrophilic polysulfone membrane using polyacrylic acid with polyvinyl pyrrolidone", *J. Appl. Polymer Sci.*, **132**(22). DOI: 10.1002/app.41964
- Sinha, M.K. and Purkait, M.K. (2013), "Increase in hydrophilicity of polysulfone membrane using polyethylene glycol methyl ether", *J. Membr. Sci.*, **437**, 7-16.
- Sinha, M.K. and Purkait, M.K. (2014a), "Enhancement of hydrophilicity of poly(vinylidene fluoride-co-hexafluoropropylene) (PVDF-HFP) membrane using various alcohols as nonsolvent additives", *Desalination*, **338**(2), 106-114.
- Sinha, M.K. and Purkait, M.K. (2014b), "Preparation and characterization of novel pegylated hydrophilic pH responsive polysulfone ultrafiltration membrane", *J. Membr. Sci.*, **464**(14), 20-32.
- Sinha, M.K. and Purkait, M.K. (2015), "Preparation of fouling resistant PSF flat sheet UF membrane using amphiphilic polyurethane macromolecules", *Desalination*, **355**(1), 155-168.
- Sivakumar, M., Malaisamy, M.R., Sajitha, C.J., Mohan, D., Mohan, V. and Rangarajan, R. (1999), "Ultrafiltration application of cellulose acetate–polyurethane blend membranes", *Eur. Polym. J.*, **35**(9), 1647-1651.
- Tsai, D.H., DelRio, F.W., Keene, A.M., Tyner, K.M., Mac Cusprie, R.I., Cho, T.J., Zachariah, M.R. and Hackley, V.A. (2011), "Adsorption and conformation of serum albumin protein on gold nanoparticles investigated using dimensional measurements and in situ spectroscopic methods", *Langmuir*, **27**(6), 2464-2477.
- Wang, D.M., Lin, F.C., Wu, T.T. and Lai, J.Y. (1998), "Formation mechanism of the macrovoids induced by surfactant additives", *J. Membr. Sci.*, **142**(2), 191-204.
- Wei, X., Wang, Z., Wang, J. and Wang, S. (2012), "Novel method of surface modification to polysulfone ultrafiltration membrane by preadsorption of citric acid or sodium bisulfate", *Membr. Water Treat., Int. J.*, **3**(1), 35-49.
- Yalkowsky, S.H. and He, Y. (2010), *Handbook of Aqueous Solubility Data*, (2nd Edition), 100 p.
- Yan, X., He, G., Gu, S., Wua, X., Dua, L. and Wang, Y. (2012), "Imidazolium-functionalized polysulfone hydroxide exchange membranes for potential applications in alkaline membrane direct alcohol fuel cells", *Int. J. Hydrog. Energy*, **37**(6), 5216-5224.
- Zhang, Y., Shana, L., Tua, Z. and Zhang, Y. (2008), "Preparation and characterization of novel Ce doped non stoichiometric nano silica/polysulfone composite membranes", *Sep. Purif. Technol.*, **63**(1), 207-212.

### **List of abbreviations**

AA	Acrylic acid
AFM	atomic force microscopy
BSA	bovine serum albumin
CA	contact angle
CF	compaction factor
D-TA	dextro-tartaric acid
DL-TA	racemic tartaric acid
EWC	equilibrium water content
FESEM	field emission scanning electron microscope
HPCT	Hydrophilicity
IEC	ion exchange capacity
IEP	isoelectric point
MF	Microfiltration
PEG	polyethylene glycol
PSn	Polysulfone
PU	Polyurethane
PVP	polyvinyl pyrrolidone
PWF	pure water flux
SEM	scanning electron microscope
UF	ultrafiltration